Bull. Chem. Soc. Jpn., 70, 1649—1657 (1997)

Side-Chain Liquid-Crystalline Polyoxetanes with a Spacer-Separated Azobenzene Moiety. III.[1] Preparation and Characterization of Polyoxetanes Anchoring the Mesogen Cores of a *p*-Spacer-Substituted Phenyl 4-(4-Alkoxyphenylazo)benzoate in the Side Chain

Hiroshi Ogawa, Shigeyoshi Kanoh, and Masatoshi Motoi*

Department of Chemistry and Chemical Engineering, Faculty of Engineering, Kanazawa University, 2-40-20 Kodatsuno, Kanazawa 920

(Received December 24, 1996)

Polyoxetanes anchoring the mesogen cores of *p*-spacer-substituted phenyl 4-(4-alkoxyphenylazo)benzoates through a pendant spacer, $-CH_2O(CH_2)_4O-$, were prepared by a BF_3-initiated cationic ring-opening polymerization of the corresponding oxetanes, followed by a fractional reprecipitation of the raw polymer products containing oligomer fractions. The polyoxetanes separated from the oligomers had their peak tops at molecular weights of around 10000—23000 in nearly mono- or dimodal molecular-weight dispersity curves determined by gel permeation chromatography, and indicated fan-shaped textures due to a smectic mesophase over a wide temperature range from about 250 °C to room temperature on heating and cooling processes by polarized optical microscopy. The formation of highly ordered assemblies of the pendant mesogens is ascribable to a cohesion of the 4-(4-alkoxyphenylazo)benzoate moiety in the mesogen core, which can form a larger dipole, due to forming a longer conjugated system from the ester carbonyl to the alkoxy tail, than that of the simple 4-alkoxybenzoate moiety of the mesogen core previously reported by us.

A polyoxetane is thought by us to have several desirable properties due to a polyether linkage. Thus, a series of investigations is continuing in order to apply polyoxetane to polymer matrices that give well-found surroundings where the pendant spacer-anchored functioning species can act smoothly. In one of our several applications, the backbone of polyoxetanes derived from oxetanes **1a**—**1d** and **2a**—**2d**, as shown in Scheme 1, were found to be usable as the main chain of thermotropic side-chain liquid-crystalline polymers.[2,3]

When the pendant mesogen of the side-chain contains only the azobenzene moiety, as shown in poly(**1**)s, their mesomorphic temperature ranges were narrow, while poly(**2**)s containing both of the azobenzene and benzoate moieties in the pendant mesogen showed considerably wide mesomorphic temperature ranges. It was thus suggested that the benzoate moiety was an important segment for designing side-chain liquid-crystalline polyoxetanes, which gave a stable mesophase over a wide temperature range. Recently a polyoxetane with the butoxy tail in the pendant mesogen, prepared as a member of poly(**3**)s, was also found to comprise thermotropic side-chain liquid-crystalline polymers; these findings were briefly reported in our previous paper.[4] Lu and Hsu also prepared side-chain liquid-crystalline polyoxetanes, which showed the formation of a liquid-crystalline state identified as being smectic mesophases of the S_A, S_B, and S_G types, using *trans*-4-alkyl-1-cyclohexanecarboxylic acids as the acid component of the *p*-spacer-substituted phenyl ester, analogous to the pendant phenyl benzoate of poly(**3**)s.[5]

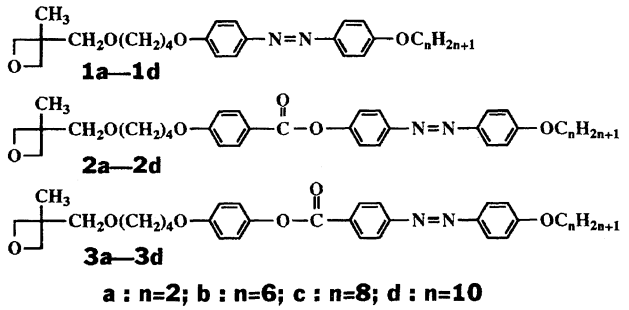

Scheme 1. Oxetane monomers used in the present study.

In this report we describe the preparation and characterization of poly(**3**)s derived from oxetanes **3a**—**3d** with differing tail lengths, since these polyoxetanes were found to be thermotropic side-chain liquid-crystalline polymers showing stable smectic mesophases, as confirmed from their fan-shaped textures, over a wide temperature range from room temperature up to 270 °C by differential scanning calorimetry (DSC) and polarized optical microscopy (POM), although the polymers of Lu and Hsu showed their mesophases below about 126°. Therefore, comparing the core structures among these ester-type polymers is required in order to understand the effect of the aromatic ester on the appearance of mesophases

and their thermal stability. Especially, in a comparison between poly(**3**)s and poly(**2**)s with the same tails, the influence of the pendant mesogens on the mesophase structures may be discussed simply without respect to another influence exerted by the polyoxetane backbones, since the structural formulas of these isomeric polymers are different from each other only in the direction of the ester bonding between the azobenzene aromatic ring and the spacer-linked benzene ring.

Results and Discussion

Oxetanes and Their Polymers. Oxetanes **3a**—**3d** and their polymers were prepared through the synthetic route shown in Scheme 2. The terminal bromine atom of the side chain of oxetane **4** was converted to a *p*-substituted phenol residue by a reaction of the bromide with a 3-fold molar amount of hydroquinone in the presence of potassium carbonate in *N*,*N*-dimethylformamide (DMF) according to a method reported in our previous paper.[4] The resultant *p*-substituted phenol was esterified with 4-(4-alkoxyphenylazo)-benzoic acid in the presence of dicyclohexylcarbodiimide (DCC) and 4-dimethylaminopyridine (DMAP). Raw polymer products were obtained in conversions of 70—90% from the oxetanes by their cationic ring-opening polymerization with a 0.08 molar amount of a diethyl ether–boron trifluoride (1/1) complex ($Et_2O{\cdot}BF_3$) as an initiator, followed by precipitating the reaction mixture once or twice with a solvent–precipitant system of dichloromethane (DCM)–methanol. In each case, however, the raw product contained an oligomer fraction in 24—37% of the total area of the gel permeation chromatography (GPC) curve. Generally, it is known that cyclic oligomers containing a cyclic tetramer as a main fraction are produced in a cationic ring-opening polymerization of oxetane and 3,3-dimethyloxetane, although the amount and type of cyclic oligomers produced is dependent on the polymerization conditions, such as the initiating system, temperature, monomer concentration, and solvent.[6,7] The high preference to form a cyclic tetramer could be ascribed to the preferred polymer backbone conformation.[7] The oligomer fractions produced in the present study were removed by a further reprecipitation with a tetrahydrofuran (THF)–diethyl ether system, although the resulting high-molecular-weight fractions were obtained in considerably reduced yields of 24—35%. The high-molecular-weight fractions showed their peak tops at GPC-average molecular weights (M_{gpc}) of around 10000 to 23000 in the nearly mono- or dimodal molecular weight dispersity curves, as estimated by a GPC calibration curve relative to the polystyrene standards. These results are summarized in Table 1 and Fig. 1.

The ^1H NMR spectra of monomer **3d** and its polymer are exemplified in Fig. 2 together with that of poly(**2d**). In the spectrum of **3d**, the methylene protons of the oxetane ring clearly indicate an AB-quartet signal at $\delta = 4.3$—4.6, and the aromatic protons show their signals at $\delta = 6.9$—8.3 in a pattern like an AB-quartet. In the spectrum of poly(**3d**), however, the signals of the methyl and methylene groups adjacent to the quaternary carbon of the main chain appear at the ordinary chemical-shift values, which are lower than those for the protons (H^c, H^f, and H^j) of the corresponding methyl and methylene groups in monomer **3d**. Such a change in the chemical-shift values was also observed for the conversion of **2d** to poly(**2d**). This sifting of the signals in the NMR spectra showed before and after ring-opening of an oxetane ring, in general, may also be interpreted on the basis of the effect of an *s* character enhanced, to a more or less

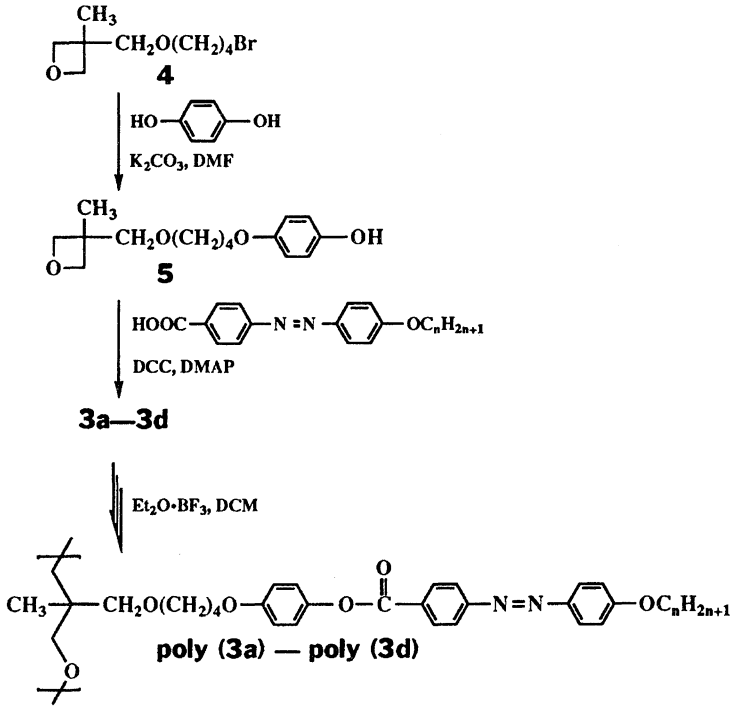

Scheme 2. A synthetic route of oxetanes, **3a**—**3d**, and their polymers.

Table 1. Polyoxetanes Obtained by Ring-Opening Polymerization with $Et_2O{\cdot}BF_3$ [a]

			Raw product polymers[b]		Poly(3)s[c]
	n in	$[M]_0$[d]	Yield	Oligomer[e]	Yield
Monomer	tail	mol dm^{-3}	%	%	%
3a	2	0.38	63	37	35
3b	6	0.27	83	30	30
3c	8	0.33	76	32	24
3d	10	0.32[f]	75	24	36

a) Carried out in DCM at rt for 50 h using a 0.08 molar amount of BF_3 with respect to monomer. b) Raw product polymers obtained by pre-reprecipitation with a DCM–methanol system. c) High-molecular-weight fractions obtained by post-reprecipitation of the raw product polymers with a THF–ether system. d) Initial monomer concentration. e) Fraction of oligomers in the product polymer is indicated in % for the total of the GPC curve. f) Toluene was used as a solvent.

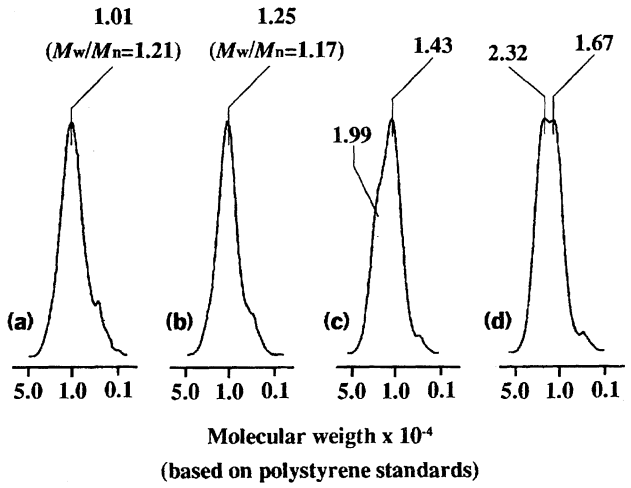

Fig. 1. GPC chromatograms of (a) poly(**3a**), (b) poly(**3b**), (c) poly(**3c**), and (d) poly(**3d**). Figures at peak tops indicate molecular weights ($\times 10^{-4}$) estimated from those of polystyrene standards.

extent, for the external orbitals in three- and four-membered cycloalkanes.[8] The spectrum of poly(**3d**) resembles that of **3d**, and also resembles that of poly(**2d**), although in these polymers the aromatic protons (H^m and $H^{m'}$) located at the ortho positions of the acyloxy group indicate their signals at different chemical-shift values, i. e., the H^m of poly(**3d**) resonated by an about 0.2 ppm lower chemical shift than the $H^{m'}$ of poly(**2d**). Furthermore, the IR spectra of poly(**3**)s did not show any band at about 980 cm^{-1} due to the cyclic ether of the oxetane ring, similar to that described in the previous paper for poly(**2d**). The elemental analysis data of poly(**3**)s agreed approximately with the theoretical values (see Experimental section). Thus, the formation of the desired polyoxetanes with M_{gpc} above 10000 were confirmed.

DSC and POM of Polyoxetanes, Poly(*3*)s. DSC curves for the second heating and first cooling scans are shown in Fig. 3 for the poly(**3**)s, except for poly(**3a**). The DSC curve of poly(**3a**) was shown only on the first heating scan, since its isotropic phase transition temperature (T_i) was close to its decomposition temperature at 290—300 °C. The T_i values of the other polymers were observed at below 270 °C on the first heating, and subsequent measurements were performed well upon the cooling and heating scans.

Photomicrographs of the samples, prepared by sandwiching each of the poly(**3**)s between two coverglasses, were taken at appropriate temperatures by POM. Several of these textures are exemplified in Fig. 4. All of the photomicrographs obtained in this work indicated fan-shaped textures, as exemplified by typical textures (A, C, E, and G) and identified as the smectic mesophase over a great part of the mesomorphic temperature range. However, the appearance of bâtnnets was observed at a temperature of around T_i (texture F), and the fans were banded or striated in a lower temperature range (textures B, D, and I). In the DSC curves of poly(**3b**), poly(**3c**), and poly(**3d**), exo- or endothermic peaks are observed at 80—110 °C in enthalpies of about 1.2—5.4 J g^{-1}. The appearance of these peaks is not ascribable to a mesomorphic phase transition, since no distinctive change in the POM texture was observed at the corresponding temperature; however, these thermic peaks may be ascribed to the occurrence of a conformational change or crystallization in parts of the polyoxetane main chains, which are separated from the mesophase domains formed with the mesogenic side chains. Three types of conformations have so far been found for poly(oxytrimethylene) and polyoxetane main chains with non-mesogenic side chains.[9,10]

The DSC curves of monomers **3a**—**3d** are also shown in Fig. 5, and several of their textures are exemplified in Fig. 6. In these DSC curves, sharp peak with enthalpies of 4—20 J g^{-1} appeared at lowered temperatures of around 30—90 °C, and in a few cases a distinctive change in the texture was observed at these temperatures. Upon the first cooling process for **3a**, the isotropic phase-like texture (J) changed at 45 °C to a texture (K) analogous to what is often observed when lamellated polymers form spherulitic crystals, presumably indicating the formation of a crystalline structure of the monomer. On the first cooling process for **3d**, the change from an isotropic phase-like texture to the mosaic schlieren texture (L) was observed at 70 °C; then, spots appeared over texture L, as shown by texture M, indicating an initial generation stage of another mesophase. Thus, poly(**3**)s tended to give a stable mesophase showing a fan-shaped texture, while the mesophases and textures of the corresponding monomers tended to be influenced by their tail length. Additionally, on second heating scans of **3a**, **3c**, and **3d**, exothermic peaks were observed at 60—70 °C, while the corresponding polymers did not show any exothermic peaks on the heating scans. It is not yet clear, however, what phase-transition the appearance of the exothermic peaks on heating scan is ascribed to. It is at least suggested by these findings that the polyoxetane main chain immobilizing the pendant mesogens favors the appearance and maintenance of a mesophase, although the oxetane linked to the mesogen does not necessarily do so.

As shown in Fig. 4, by a comparison between POM textures G and H for poly(**3d**) and its raw polymer, respectively, the results of the above-mentioned POM measurement for

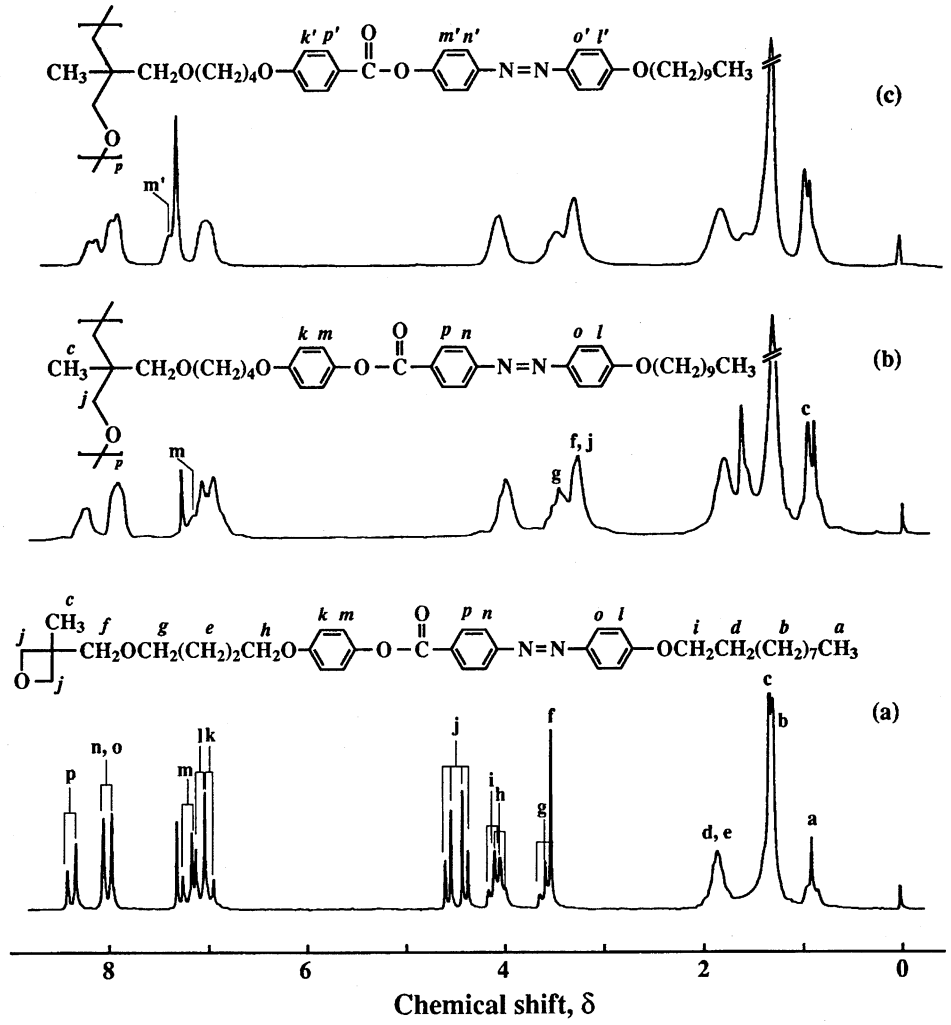

Fig. 2. ^{1}H NMR spectra of (a) **3d**, (b) poly(**3d**), and (c) poly(**2d**).

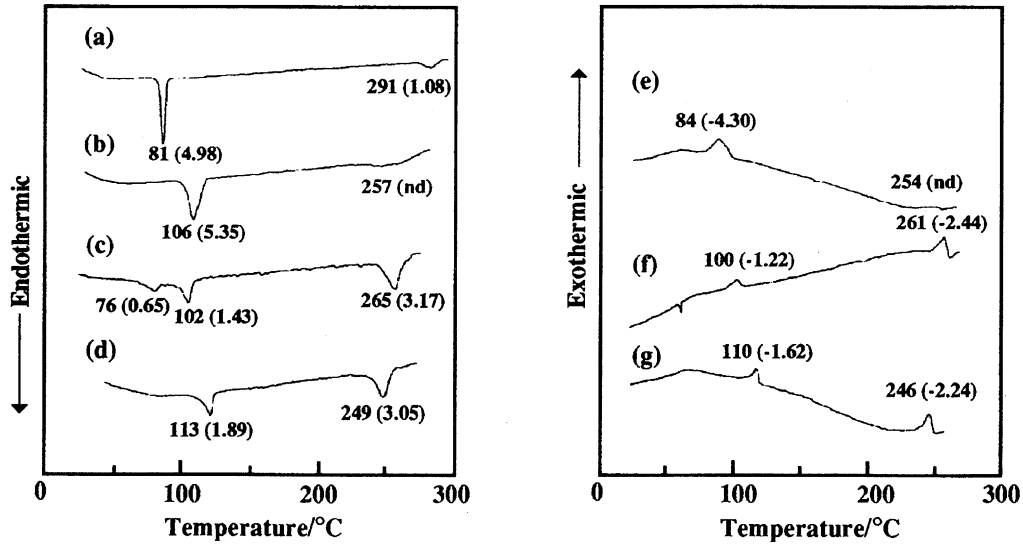

Fig. 3. DSC curves of poly(**3**)s on 2nd heating (left), and 1st cooling scans (right): (a) on 1st heating of poly(**3a**); (b) and (e) poly(**3b**); (c) and (f) poly(**3c**); (d) and (g) poly(**3d**). Figures at thermal peaks indicate temperature, and their enthalpies are given in parentheses. In each scan, an arbitrary scale was used for heat flow (mW) in the ordinate.

poly(**3**)s were similarly given for their raw polymers, although their T_i values were by 10—20 °C lower than those of poly(**3**)s. As described in our previous report, poly(**2**)s were also obtained as their raw polymers, which had a peak

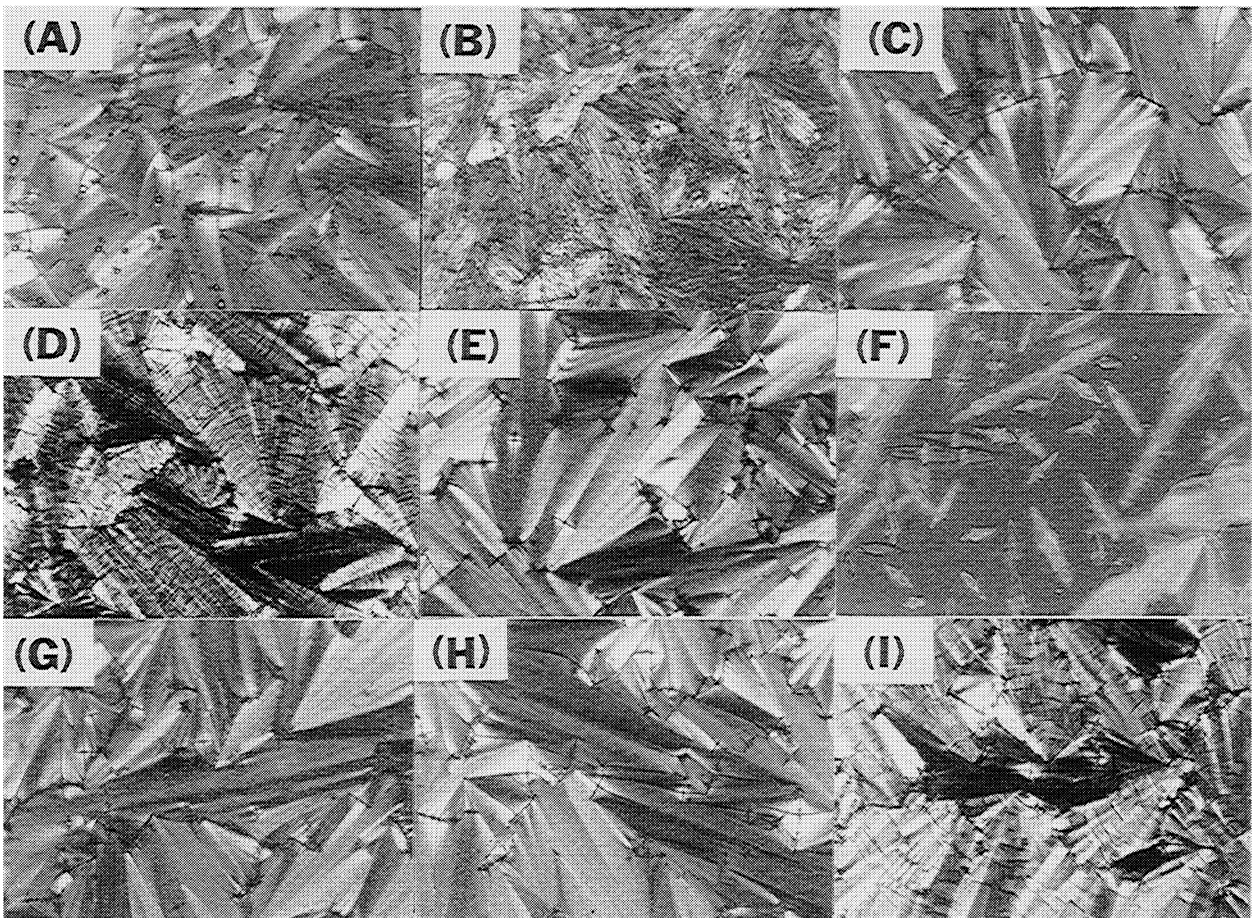

Fig. 4. Photomicrographs (magnification 200×) of polyoxetanes taken by POM at appropriate temperatures on 1st cooling process for (A)—(C) and (F)—(I) and on 2nd heating process for (D) and (E). Poly(**3a**): (A) 176 and (B) 22 °C; Poly(**3b**): (C) 105 °C; Poly(**3c**): (D) 22 and (E) 155 °C; Poly(**3d**): (F) 253, (G) 208, (H) 218 (for the raw polymer of poly(**3d**)), and (I) 19 °C.

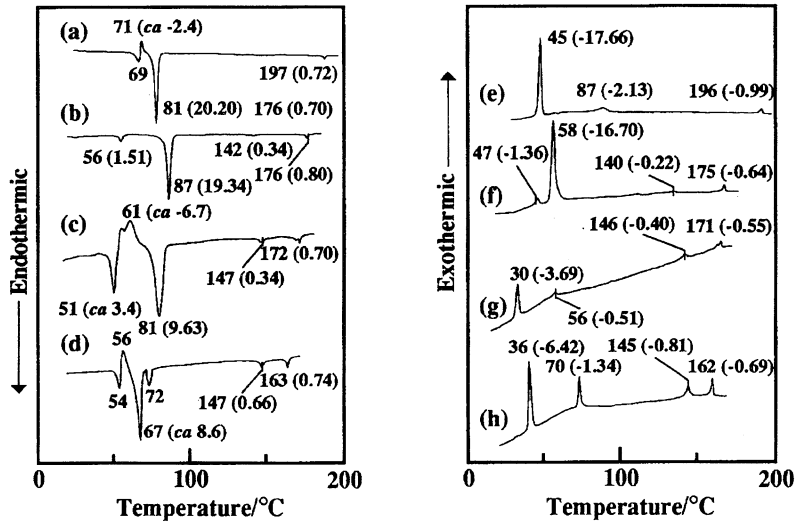

Fig. 5. DSC curves of monomers **3a**—**3d** on 2nd heating (left) and 1st cooling scans (right): (a) and (e) **3a**; (b) and (f) **3b**; (c) and (g) **3c**; (d) and (h) **3d**. Figures at thermal peaks indicate temperature, and their enthalpies are given in parentheses. In each scan, an arbitrary scale was used for heat flow (mW) in the ordinate.

top of the main fraction at M_{gpc} 8000—27000 in the GPC curve and contained the oligomer fraction in 13—24% of the total area of the GPC curve, since the high-molecular-weight fraction was not yet obtained, as in the case of obtaining poly(**3**)s by post-reprecipitation. However, these poly(**2**)s indicated POM textures different from the observed fan-shaped textures, even for the raw polymers of poly(**3**)s, as outlined in the following. The poly(**2**)s carrying shorter

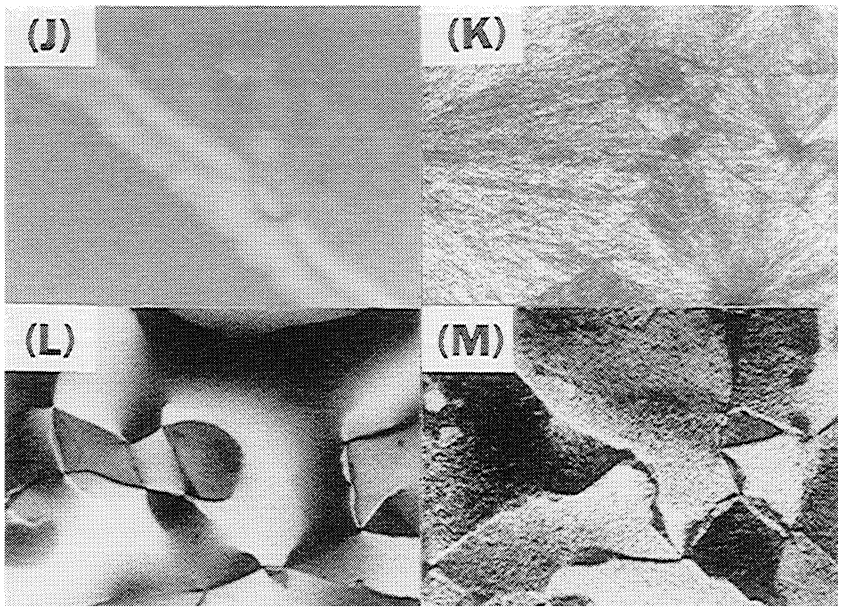

Fig. 6. Photomicrographs (magnification 200×) of oxetanes, **3a**, and **3d**, taken by POM at appropriate temperatures on 2nd heating process for (J) and on 1st cooling process for (K)—(M). **3a**: (J) 189 °C (a texture due to an isotropic phase appears in the bottom left area and a texture due to a nematic texture in the upper right area) and (K) 26 °C; **3d**: (L) 64 and (M) 38 °C.

tails from methoxy to propoxy groups indicated the schlieren texture due to the formation of the nematic mesophase over a wide temperature range from about 250 °C to room temperature. The polymers carrying longer tails from the octyloxy to the dodecyloxy groups showed a fan-shaped texture due to the formation of smectic mesophase over most of the mesomorphic temperature range. Upon lowering the temperature this fan-shaped texture changed to a texture of banded focalconic fans. When the polymers had moderately long tails, such as butoxy to hexyloxy groups, their textures showed a schlieren pattern followed by a bunch-like pattern in the higher temperature range, and then a broken fan-shaped pattern in the lower temperature range.[3] Thus, the core structure of poly(**3**)s plays an important role to form highly ordered mesophases, since the polymers of **3**s gave fan-shaped textures due to the smectic mesophase, even when containing the oligomer fraction, while, in poly(**2**)s, the formation of mesophases was influenced by the tail length or the existence of the oligomer fraction in the polymer.

X-Ray diffraction charts of poly(**3a**), poly(**3d**), and poly(**2d**) were taken using samples obtained by cooling the polymers to room temperature on the above-described POM measurement, as shown in Fig. 7. Obviously, the X-ray diffraction patterns indicate that poly(**3**)s have layer structures formed in their smectic mesophases, even at room temperature, and that poly(**2d**) also has such a layer structure in spite of using a raw polymer, which had a peak top of the main fraction at M_{gpc} 27000 and contained the oligomer fraction in 14% of the total area of the GPC curve. Furthermore, for poly(**3d**) a considerably high degree of ordering of the pendant mesogens in the minor axis was estimated, as indicated by the very intensive X-ray diffraction line at $2\theta = 21.0°$.

As shown in the ^{1}H NMR spectra in Fig. 2, the aromatic proton (H^m) of poly(**3d**) resonated at a chemical-shift value about 0.2 ppm lower than that of the $H^{m\prime}$ of poly(**2d**), indicating that the ether-like oxygen atom of the ester of poly(**3d**) tends to have a positive mesomery effect, although that of poly(**2d**) has such an effect to a less extent; the *m*-protons of azobenzene resonated at $\delta = 7.4$—7.6. In poly(**3d**), since the ester carbonyl group lies in a long conjugation system through π electrons of the 4-(4-alkoxyphenylazo)benzoyl moiety (Scheme 3), it attracts an electron from the ether-like oxygen atom to a less extent, compared with the carbonyl in poly(**2d**). Such a difference in the chemical shifts was observed for the other pairs of poly(**3d**)s with poly(**2d**)s used in this study. These results suggest that the longer, polar, plate-like structure of the aromatic core in poly(**3**)s favors highly ordered assemblies of the pendant mesogens, compared with the core structure of poly(**2**)s.

As above-mentioned, the pendant *trans*-4-alkyl-1-cyclohexanecarboxylates were also effective as a mesogen core, based on the same polyoxetane main chains as that of poly(**3**)s. However, polyoxetanes having aliphatic acyl cores with alkyl tails of C_nH_{2n+1} ($n = 3$—6 and 12) showed their T_i values at 53—120 °C, which were remarkably lowered from the T_i values of 210—270 °C shown for poly(**3**)s and poly(**2**)s, and indicated enthalpy values of 0.1—12 J g^{-1} at T_i, which were almost close to or higher than 0.1—3.2 J g^{-1} for poly(**3**)s and poly(**2**)s. Since the 4-alkyl-1-cyclohexylcarbonyls lack the plate-like, long conjugated system, such as in poly(**3**)s, the dipole–dipole attractive forced of the aliphatic acyl cores can not exert more efficiently to the assembly of the cores, compared with those of the 4-(4-alkoxyphenylazo)benzoyls; presumably, a smaller entropy change is estimated for the isotropic phase transition of the aromatic acyl cores than for that of aliphatic ones. Furthermore, in poly(**3**)s and even in their raw polymers, the appearance of highly ordered

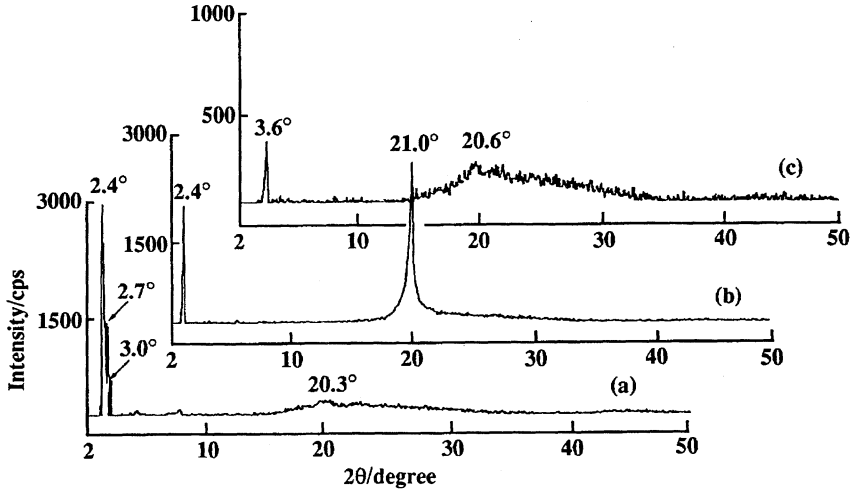

Fig. 7. X-Ray diffraction patterns of (a) poly(**3a**), (b) poly(**3d**), and (c) poly(**2d**).

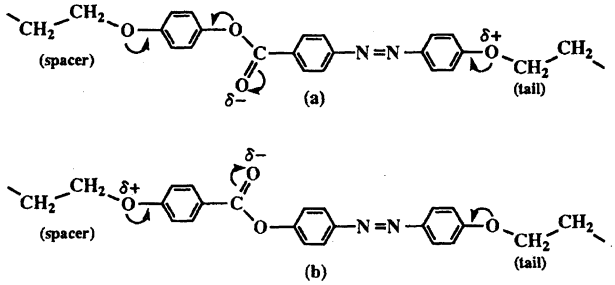

Scheme 3. Structures considered for the pendant mesogen cores of (a) poly(**3**)s and (b) poly(**2**)s.

mesophases, as shown by the fan-shaped texture, over a wide mesomorphic temperature range was not influenced by the tail length; in poly(**2**)s, however, the tail length was considered to be one of the factors which influence the formation of a mesophase (vaide ante). Thus, the plate-like, polar aromatic core of poly(**3**)s is the desired segment for packing the pendant mesogens smoothly in a highly ordered liquid-crystalline state, even at a higher temperature.

In conclusion, the *p*-spacer-substituted phenyl 4-(4-alkoxyphenylazo)benzoate moiety of poly(**3**)s was found to be a good pendant mesogen core based on the polyoxetane main chain. These polyoxetanes were readily obtained, but in considerably low yields, by the cationic ring-opening polymerization of the corresponding oxetane monomers with a 0.08 molar amount of an $Et_2O{\cdot}BF_3$ initiator, followed by post-reprecipitation of the raw polymer products obtained by the pre-reprecipitation. All of the purified polymers indicated fan-shaped textures due to the smectic mesophase over a wide temperature range from about 270 °C to room temperature, as confirmed by DSC, POM, and X-ray diffraction. In the formation of such a stable mesophase, the 4-(4-alkoxyphenylazo)benzoyls effectively act as a plate-like, polar segment of the pendant mesogens, as considered by comparing the conjugating systems of the core segments between poly(**3**)s and poly(**2**)s. Although a few of the corresponding monomers were also confirmed to be liquid-crystalline substances, the highly ordered assemblies of mesogens were smoothly achieved by immobilizing the mesogens to the polyoxetane chain, rather than to the oxetane ring. Thus, the polyoxetanes may be promising as one of polymeric supports of liquid-crystalline substances. Although the influence of the oligomer fraction in the high-molecular-weight fraction on the formation of mesophases was not considered in detail in the present study, this problem is also of interest to us from the viewpoint of knowing the role of the pendant mesogens of the high-molecular-weight fraction on the growing mechanism of a liquid-crystalline state in a mixture of these different fractions.

Experimental

Materials. **4-{4-[(3-Methyl-3-oxetanyl)methoxy]butoxy}phenol (5):**[4] Bromide **4** (21.1 mmol) was stirred with hydroquinone (63.3 mmol) in DMF (20 cm^3) at 85 °C for 10 h in the presence of K_2CO_3 (14.8 mmol). The DMF solvent was evaporated, and the residue was shaken successively with ether and 10% NaOH. The aqueous layer was acidified at pH 4 with aqueous HCl and extracted with ether. The raw product, obtained by evaporating the solvent, was washed several times with hot water until the product indicated one spot on TLC: Yield 53%; mp 81.0—82.5 °C; IR (KBr) 3300 (phenolic OH), 3070, 3050, 1520, 1480, and 830 (1, 4-disubstituted benzene), 1235 and 1020 (aromatic ether), 1130 (acyclic ether), and 980 and 840 cm^{-1} (cyclic ether); ^{1}H NMR ($CDCl_3$) δ = 1.31 (3H, s, CH_3), 1.6—2.0 [4H, m, $OCH_2(C\underline{H}_2)_2CH_2O$], 3.4—3.7 [total 4H: s, δ = 3.48, $C\underline{H}_2O(CH_2)_4O$; t, δ = 3.53, J = 5.70 Hz, $CH_2OC\underline{H}_2(CH_2)_3O$], 3.92 (2H, t, J = 5.74 Hz, $C\underline{H}_2OAr$), 4.36 and 4.53 (each 2H, AB-q, J = 5.74 Hz, CH_2 of the oxetane ring), 5.17 (1H, s, OH), and 6.75 (4H, s-like, ArH).

4-{4-[(3-Methyl-3-oxetanyl)methoxy]butoxy}phenyl 4-(4-Ethoxyphenylazo)benzoate (3a): To a solution of the phenol **5** (2.06 mmol), 4-(4-ethoxyphenylazo)benzoic acid (2.06 mmol), and DMAP (0.21 mmol) in 15 cm^3 of tetrahydrofuran (THF) DCC (2.06 mmol) was added at 0 °C. The solution was stirred at this temperature for 3 h and then at rt for 7 h. The *N,N'*-dicyclohexylurea was removed by filtration, and the THF solvent was evaporated off from the filtrate. The remaining solid was extracted with DCM and washed three times with saturated aqueous $NaHCO_3$. The crude product was purified by column chromatography on silica gel with chloroform as the eluent, and then recrystallized from ethanol (see Fig. 5 for mp): Yield 22%; IR (KBr) 3070, 3050, 1600, 1580, 1500, and 840 (1,4-disubstituted benzene), 1730, 1270, 1190

(ester), 1255 and 1075 (aromatic ether), 1110 (acyclic ether), and 980 cm^{-1} (cyclic ether); ^1H NMR ($CDCl_3$) $\delta = 1.32$ (3H, s, CH_3 of the oxetane ring), 1.47 (3H, t, $J = 7.08$ Hz, $OCH_2C\underline{H}_3$), 1.6—1.8 [4H, m, $OCH_2(C\underline{H}_2)_2CH_2O$], 3.4—3.7 [total 4H: s, $\delta = 3.50$, $C\underline{H}_2O(CH_2)_4O$; t, $\delta = 3.55$, $J = 5.62$ Hz, $CH_2OC\underline{H}_2(CH_2)_3O$], 3.9—4.3 [total 4H: t, $\delta = 4.00$, $J = 6.34$ Hz, $O(CH_2)_3C\underline{H}_2OAr$; q, $\delta = 4.14$, $J = 7.00$ Hz, $OC\underline{H}_2CH_3$], 4.37 and 4.52 (each 2H, AB-q, $J = 5.86$ Hz, CH_2 of the oxetane ring), and 6.93—8.31 (total 12H: AB-q-like, $\delta = 6.93$ and 7.15, $J = 9.03$ Hz, $OC_6\underline{H}_4OCOAr$; AB-q-like, $\delta = 7.02$ and 7.96, $J = 8.79$ Hz, $ArN_2C_6\underline{H}_4OC_2H_5$; AB-q-like, $\delta = 7.96$ and 8.31, $J = 8.30$ Hz, $OCOC_6\underline{H}_4N_2Ar$).

Found: C, 69.41; H, 6.67; N, 6.04%. Calcd for $C_{30}H_{34}N_2O_6$: C, 69.48; H, 6.61; N, 5.40%.

4-{4-[(3-Methyl-3-oxetanyl)methoxy]butoxy}phenyl 4-[4-(Hexyloxy)phenylazo]benzoate (3b): Obtained in a 28% yield in the same manner as the preparation of **3a**; see Fig. 5 for mp; IR (KBr) 3070, 3050, 1600, 1580, 1510, and 840 (1,4-disubstituted benzene), 1725, 1275, and 1200 (ester), 1255 and 1080 (aromatic ether), 1125 and 1110 (acyclic ether), and 980 cm^{-1} (cyclic ether); ^1H NMR ($CDCl_3$) $\delta = 0.92$ [3H, t-like, $O(CH_2)_5C\underline{H}_3$], 1.2—1.5 [total 9H: s, $\delta = 1.32$, CH_3; m, $O(CH_2)_2(C\underline{H}_2)_3CH_3$] 1.6—2.0 [total 6H: m, $OCH_2(C\underline{H}_2)_2CH_2O$ and $OCH_2C\underline{H}_2C_4H_9$], 3.4—3.7 (total 4H: s, $\delta = 3.50$; t, $\delta = 3.55$, $J = 5.40$ Hz), 3.9—4.2 (total 4H: t, $\delta = 4.00$, $J = 5.37$ Hz; t, $\delta = 4.06$, $J = 6.40$ Hz, $OC\underline{H}_2C_5H_{11}$), 4.36 and 4.52 (each 2H, AB-q, $J = 5.86$ Hz), and 6.95—8.31 (total 12 H: AB-q-like, $\delta = 6.95$ and 7.14, $J = 9.04$ Hz; AB-q-like, $\delta = 7.02$ and 7.96, $J = 8.30$ Hz; AB-q-like, $\delta = 7.96$ and 8.31, $J = 8.55$ Hz).

Found: C, 70.96; H, 7.37; N, 5.00%. Calcd for $C_{34}H_{42}N_2O_6$: C, 71.06; H, 7.37; N, 4.87%.

4-{4-[(3-Methyl-3-oxetanyl)methoxy]butoxy}phenyl 4-[4-(Octyloxy)phenylazo]benzoate (3c): Obtained in a 39% yield in the same manner as the preparation of **3a**; see Fig. 5 for mp; IR (KBr) 3080, 3050, 1600, 1580, 1510, and 840 (1,4-disubstituted benzene), 1730, 1275, and 1200 (ester), 1250 and 1085 (aromatic ether), 1140 and 1105 (acyclic ether), and 980 cm^{-1} (cyclic ether); ^1H NMR ($CDCl_3$) $\delta = 0.90$ [3H, t-like, $O(CH_2)_7C\underline{H}_3$], 1.1—1.5 [total 13H: s, $\delta = 1.32$; m, $O(CH_2)_2(C\underline{H}_2)_5CH_3$], 1.7—2.0 [total 6H: m, $OCH_2(C\underline{H}_2)_2CH_2O$ and $OCH_2C\underline{H}_2C_6H_{13}$], 3.4—3.7 (total 4H: s, $\delta = 3.50$; t, $\delta = 3.55$, $J = 5.40$ Hz), 4.01 (2H, t, $J = 5.37$ Hz), 4.06 (2H, t, $J = 6.59$ Hz, $OC\underline{H}_2C_7H_{15}$), 4.37 and 4.52 (each 2H, AB-q, $J = 5.86$ Hz), and 6.96—8.31 (total 12H: AB-q-like, $\delta = 6.96$ and 7.13, $J = 9.03$ Hz; AB-q-like, $\delta = 7.01$ and 7.96, $J = 9.03$ Hz; AB-q-like, $\delta = 7.96$ and 8.31, $J = 8.55$ Hz).

Found: C, 71.45; H, 7.66; N, 4.83%. Calcd for $C_{36}H_{46}N_2O_6$: C, 71.73; H, 7.69; N, 4.65%.

4-{4-[(3-Methyl-3-oxetanyl)methoxy]butoxy}phenyl 4-[4-(Decyloxy)phenylazo]benzoate (3d): Obtained in a 44% yield in the same manner as the preparation of **3a**; see Fig. 5 for mp; IR (KBr) 3070, 3050, 1600, 1580, 1500, and 840 (1,4-disubstituted benzene), 1735, 1275, 1275 and 1080 (ester), 1255 and 1080 (aromatic ether), 1140 and 1105 (acyclic ether), and 980 cm^{-1} (cyclic ether); ^1H NMR ($CDCl_3$) $\delta = 0.91$ [3H, t-like, $O(CH_2)_9C\underline{H}_3$], 1.2—1.5 [total 17H: m, $\delta = 1.32$; m, $O(CH_2)_2(C\underline{H}_2)_7CH_3$], 1.7—2.0 [total 6H: m, $OCH_2(C\underline{H}_2)_2CH_2O$ and $OCH_2C\underline{H}_2C_8H_{17}$], 3.4—3.7 (total 4H: s, $\delta = 3.50$; t, $\delta = 3.55$, $J = 5.40$ Hz), 4.01 (2H, t, $J = 5.13$ Hz), 4.06 [2H, t, $J = 6.11$ Hz, $OC\underline{H}_2(CH_2)_8CH_3$], 4.37 and 4.52 (each 2H, AB-q, $J = 5.86$ Hz), and 6.95—8.31 (total 12H: AB-q-like, $\delta = 6.95$ and 7.15, $J = 9.28$ Hz; AB-q-like, $\delta = 7.02$ and 7.96, $J = 8.79$ Hz; AB-q-like, $\delta = 7.96$ and 8.31, $J = 8.79$ Hz).

Found: C, 72.10; H, 7.94; N, 4.43%. Calcd for $C_{38}H_{50}N_2O_6$: C, 72.35; H, 7.99; N, 4.44%.

Polyoxetanes: A half of 1 g of **3** was polymerized in DCM or toluene at 25—30 °C with a 0.08 molar amount of $THF{\cdot}BF_3$ under a nitrogen atmosphere. The product polymers were reprecipitated from DCM to methanol to give the raw polymers. These were further reprecipitated from THF to ether to obtain high-molecular-weight fractions, which were dried in a vacuum.

Generally, poly(**3**)s showed the characteristic IR bands at the following wavenumbers: 1730, 1270, and 1200—1190 (ester), 1260—1255 and 1070—1060 (aromatic ether), 1110—1100 (acyclic ether), and 840 cm^{-1} (1,4-disubstituted benzene). The ^1H NMR spectra ($CDCl_3$) and elemental analysis of poly(**3**)s gave the following data.

Poly(3a): $\delta = 0.8$—1.0 [3H, CH_3 adjacent to the quaternary carbon of the main chain (s-like signal centered at $\delta = 0.95$)], 1.3—1.5 [3H, $OCH_2C\underline{H}_3$ (t-like signal centered at $\delta = 1.46$)], 1.5—2.0 [4H, $OCH_2(C\underline{H}_2)_2CH_2O$], 3.1—3.6 [8H, CH_2 adjacent to the quaternary carbon and $CH_2OC\underline{H}_2(CH_2)_3O$], 3.8—4.2 (4H, $OC\underline{H}_2CH_3$ and $CH_2O(CH_2)_3C\underline{H}_2O$), 6.7—7.2 (6H, four ArHs of the OC_6H_4OCO moiety and two ArHs *ortho* to the OC_2H_5), 7.7—8.0 (4H, four ArHs *ortho* to the azo group), and 8.1—8.3 (2H, two ArHs *ortho* to the acyl group).

Found: C, 68.61; H, 6.60; N, 5.46%. Calcd for $C_{30}H_{34}N_2O_6$: C, 69.47; H, 6.62; N, 5.40%.

Poly(3b): $\delta = 0.8$—1.0 [6H, $OC_5H_{10}C\underline{H}_3$ (a signal centered at $\delta = 0.92$) and CH_3 adjacent to the quaternary carbon of the main chain (a signal centered at $\delta = 0.95$)], 1.3—1.5 [6H, $O(CH_2)_2(C\underline{H}_2)_3CH_3$], 1.5—2.0 [6H, $OCH_2(C\underline{H}_2)_2CH_2O$ and $OCH_2C\underline{H}_2C_4H_9$], 3.1—3.6 (8H), 3.9—4.2 (4H, $OC\underline{H}_2C_5H_{11}$ and $CH_2O(CH_2)_3C\underline{H}_2O$), 6.7—7.2 (6H), 7.7—8.0 (4H), 8.1—8.3 (2H).

Found: C, 70.52; H, 7.36; N, 4.73%. Calcd for $C_{34}H_{42}N_2O_6$: C, 71.04; H, 7.38; N, 4.87%.

Poly(3c): $\delta = 0.8$—1.0 [6H, $OC_7H_{14}C\underline{H}_3$ (a signal centered at $\delta = 0.89$) and CH_3 adjacent to the quaternary carbon of the main chain (a signal centered at $\delta = 0.95$)], 1.2—1.5 [10H, $O(CH_2)_2(C\underline{H}_2)_5CH_3$], 1.5—2.0 [6H, $OCH_2(C\underline{H}_2)_2CH_2O$ and $OCH_2C\underline{H}_2C_6H_{13}$], 3.1—3.6 (8H), 3.9—4.2 (4H, $OC\underline{H}_2C_7H_{15}$ and $CH_2O(CH_2)_3C\underline{H}_2O$), 6.7—7.2 (6H), 7.7—8.0 (4H), 8.1—8.3 (2H),

Found: C, 71.29; H, 7.82; N, 4.54%. Calcd for $C_{36}H_{46}N_2O_6$: C, 71.73; H, 7.69; N, 4.65%.

Poly(3d): $\delta = 0.8$—1.0 [6H, $OC_7H_{14}C\underline{H}_3$ (a signal centered at $\delta = 0.88$) and CH_3 adjacent to the quaternary carbon of the main chain (a signal centered at $\delta = 0.95$)], 1.2—1.5 [14H, $O(CH_2)_2(C\underline{H}_2)_7CH_3$], 1.5—2.0 [6H, $OCH_2(C\underline{H}_2)_2CH_2O$ and $OCH_2C\underline{H}_2C_8H_{17}$], 3.1—3.6 (8H), 3.8—4.1 (4H, $OC\underline{H}_2C_9H_{19}$ and $CH_2O(CH_2)_3C\underline{H}_2O$), 6.7—7.2 (6H) 7.7—8.0 (4H) 8.1—8.4 (2H).

Found: C, 71.81; H, 7.92; N, 4.31%. Calcd for $C_{38}H_{50}N_2O_6$: C, 72.35; H, 7.99; N, 4.44%.

4-(4-Alkoxyphenylazo)benzoic Acids: Ethyl 4-(4-alkoxyphenylazo)benzoates were obtained by a reaction of ethyl 4-(4-hydroxyphenylazo)benzoate (11.1 mmol) with an alkyl bromide (16.7 mmol) in acetone (5 cm^3) under reflux for 10 h in the presence of K_2CO_3 (7.8 mmol) followed by recrystallization from ethanol. The yields and melting points of the esters were as follows: ethoxy: 92%, mp 119—120 °C; hexyloxy: 98%, 78.5—79.5 °C; octyloxy: 87%, mp 77.0—79.0 °C; and decyloxy: 91%, mp 99.5—100.0 °C. These esters were hydrolyzed with 2 mol dm^{-3} aqueous NaOH (22 cm^3) in methanol (22 cm^3) at reflux temperature for 6 h. After being subjected to the ordinary post-treatment, the crude products were recrystallized from acetic acid to give the desired acids in 97, 99, 76, and 97% yields, respectively, for ethoxy-, hexyloxy-, octyloxy-, and decyloxy-substituted derivatives.

Measurement. IR and ^1H NMR spectroscopy, GPC, DSC, and POM were performed in the manner described in our previous report.[2)]

References

1) Parts I and II : Refs. 2 and 3, respectively.
2) M. Motoi, K. Noguchi, A. Arano, S. Kanoh, and A. Ueyama, *Bull. Chem. Soc. Jpn.*, **66**, 1778 (1993).
3) H. Ogawa, T. Hosomi, T. Kosaka, S. Kanoh, A. Ueyama, and M. Motoi, *Bull. Chem. Soc. Jpn.*, **70**, 175 (1997).
4) T. Hiruma, K. Kanoh, T. Yamamoto, S. Kanoh, and M. Motoi, *Polym. J.*, **27**, 78 (1995).
5) Y. Lu and C. Hsu, *Macromolecules*, **28**, 1673 (1995).
6) P. Dreyfuss and M. P. Dreyfuss, *Polym. J.*, **8**, 81 (1976).
7) M. Bucquoye and E. J. Goethals, *Makromol. Chem.*, **179**, 1681 (1978).
8) J. March, "Advanced Organic Chemistry," 4th ed, J. Wiley & Sons, New York (1992), p. 152.
9) H. Tadokoro, Y. Takahashi, Y. Chatani, and H. Kakida, *Makromol. Chem.*, **109**, 96 (1967).
10) H. Kakida, D. Makino, Y. Chatani, M. Kobayashi, and H. Tadokoro, *Macromolecules*, **3**, 569 (1970).